ISSN 2032-6653

The World Electric Vehicle Journal, Vol 2, Issue 4

An At-All Operating Points Highly Efficient PMSM for HEV

Uwe Vollmer* and Uwe Schäfer*

Average losses of the electric drive throughout a driving cycle are an important issue for hybrid electric vehicles. Permanent magnet synchronous electric motors (PMSM) are the most efficient electric drives under load conditions. However, they suffer from idle losses at high speed and low load, which is a typical operating condition in highway cycles. This leads, in some cases, to even higher fuel consumption of HEV vs. conventional vehicles.

As well designed permanent magnet machines for HEV usually have excellent efficiency at operating points close to their rating, the main focus of the presented work is achieving an improvement in no load and reduced load conditions. Such losses will occur at high speed and low load, because the PMSM creates an induced voltage exceeding the battery voltage, which must be compensated by an inductive voltage drop through the motor inductance by a purely reactive current causing losses.

A proposal for a special design for PMSM with regard to the ability of active reduction of those losses at high speeds is made in the following comment: The compensation current depends on the motor inductance. Obviously, a high inductance in the axis of magnetization needs a low compensation current, whereas a low inductance in the quadrature-axis results in a large constant power range. So a special design of an asymmetrical PMSM has been developed in order to achieve minimum idle losses.

Keywords: PMSM, Field Weakening, Efficiency, Saliency, HEV

1. REASONS FOR A NEW DESIGN OF PMSM IN HEV

In most of the known hybrid car concepts the electric motor runs, at high speeds, in idle mode or low load conditions. In these operating modes a permanent magnet synchronous machine induces voltages which could be higher than the supplying battery voltage and the acceptable voltage of a dc voltage link. A reactive current to weaken the magnet flux therefore is needed to limit the induced voltage.

The benefit of this reactive current is the reduction of iron losses in the motor. Those iron losses are related to the electric frequency and the flux density in the iron parts of the motor. However a current needed for flux weakening in the motor will cause losses in the copper of the stator. Typically the iron losses will, at higher speeds, exceed the copper losses. To get the best results, with say a minimum of losses in high speed conditions, it is necessary to diminish the need of the reactive current for flux weakening purposes. Or in other words, a small reactive current should reduce the flux density in the stator iron profoundly to get a minimum in over all losses in the motor. To achieve this goal, the inductivity in the axis of magnetization (direct-axis) L_d, has to have large values.

The following picture will give an image of two motors which have only different inductances in direct-axis. In Figure 1, the vector-diagram of currents, flux-linkage and voltages are shown. The currents I_1 in both diagrams are of the same value. The inductance L_d in the top diagram has double the value of L_d in the bottom diagram.

It is easy to see that the voltage U_1 in the top diagram has a higher value compared to the bottom diagram, corresponding to the respective flux-linkage.

To obtain a wide constant power range, which is needed for a typical speed range of HEV, the inductance in the quadrature-axis L_q has to be small. In this case, currents in direction of the q-axis will produce only small reactive voltage and therefore the voltage at the motor terminals at higher speeds will not increase to values which can not be reached by an appropriate inverter.

*TU Berlin
Department for Electrical Drives
Einsteinufer 11 10587 Berlin

ISSN 2032-6653

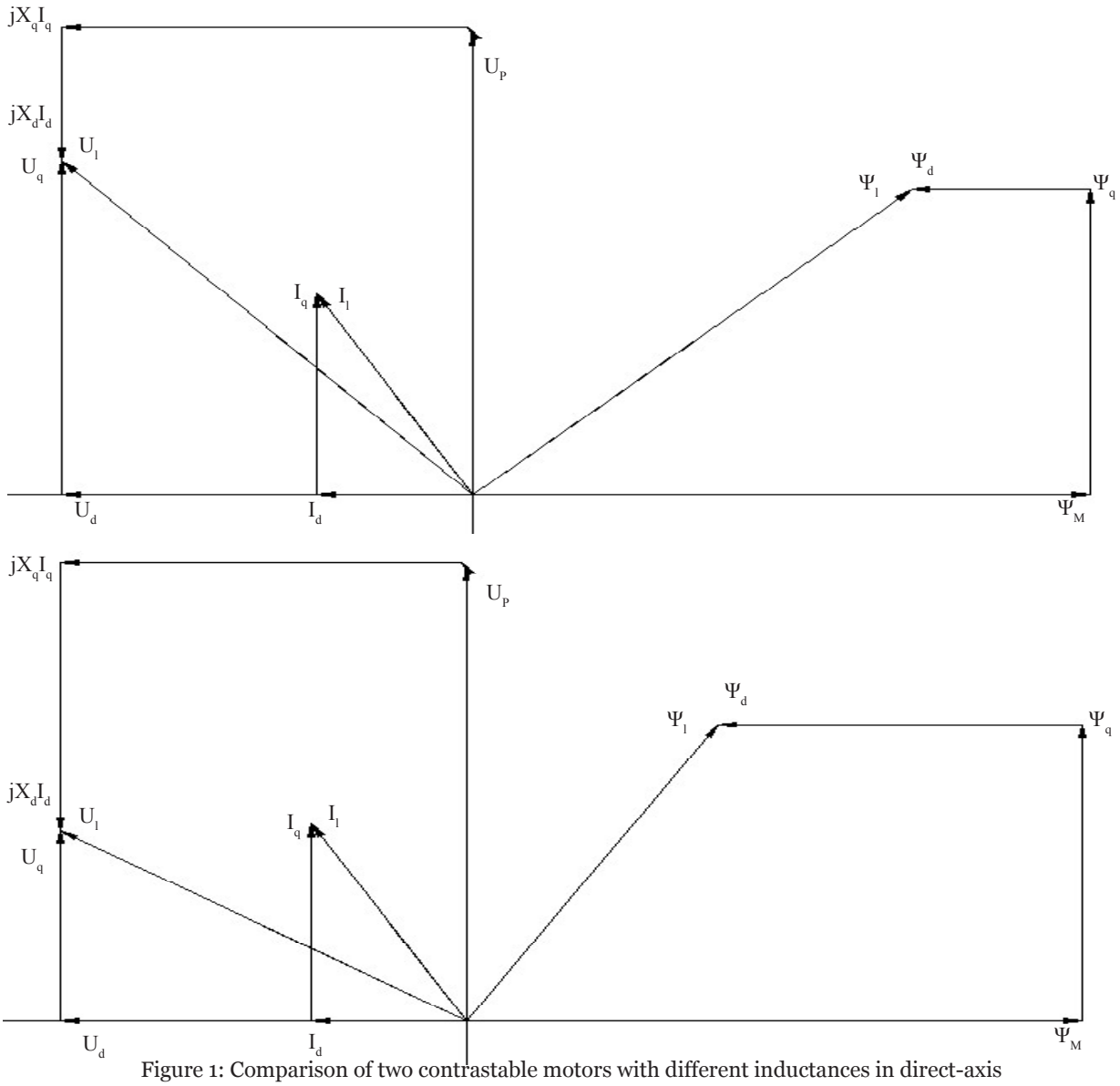

Figure 1: Comparison of two contrastable motors with different inductances in direct-axis

In the following Figure 2 the effect of different inductances in q-axis are shown in the same manner as in Figure 1. L_q in the right diagram is smaller than L_q in the left diagram.

The effect of a small inductance L_q is similar to the effect of a high inductance L_d. The amount of voltage U_1 is smaller in the right diagram at the same current I_1. A combination of both, a magnification of L_d and downsizing L_q, should give the best results in an effort to reduce the losses in the PMSM running at low load conditions or idle mode.

2. DESIGN OF A ROTOR OF PMSM WITH $L_D > L_Q$

Electrical machines with a ratio $L_d / L_q > 1$ are well known. Synchronous machines with salient poles have this ratio due to a small magnetic reluctance in direction of the magnetizing axis and a large magnetic reluctance in direction of the q-axis. The reluctance in both axes are in this case a result of the variation of the air gap in this type of machines.

The distribution of flux-density in the air gap B_δ of a salient pole machine has a special characteristic. A

ISSN 2032-6653

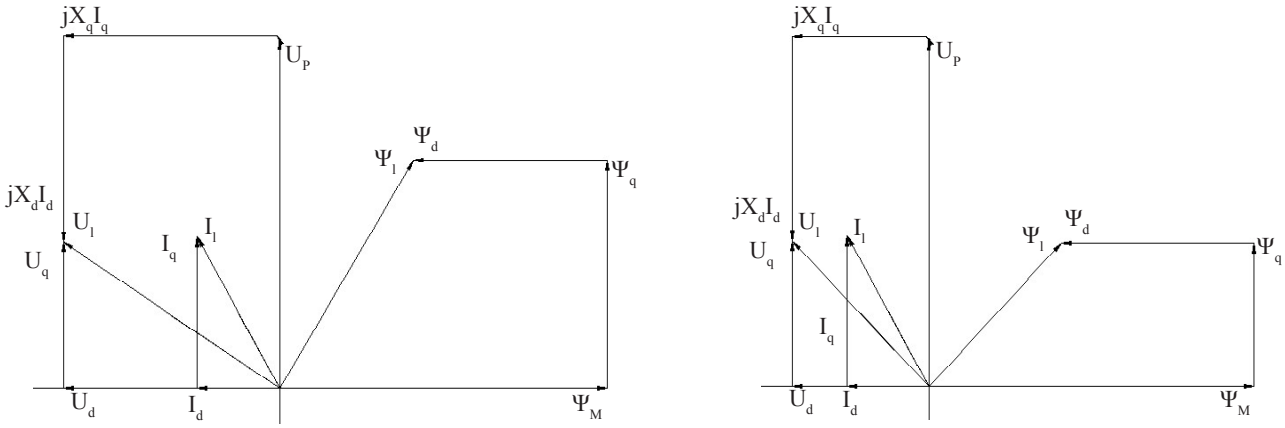

Figure 2: Comparison of two contrastable motors with different inductances in quadrature-axis

current		flux-linkage		voltage	
		Ψ_M	magnet-flux-linkage		
I_d	magnetizing current	Ψ_d	flux-link. due to I_d	U_d	direct voltage
I_q	quadrature current	Ψ_q	flux-link. due to I_q	U_q	quadrature voltage
I_1	terminal current	Ψ_1	combined flux-link.	U_1	terminal voltage

Table 1: Variables in Figure 1 and 2

Fourier-analysis shows, that the 3rd harmonic B_3 of the characteristic flux-density distribution has to have an angle of 180° in relation to the 1st harmonic B_1. In PMSM with surface mounted magnets B_3 has the same sign as the fundamental B_1.

There are different ways to come to a small reluctance in d-axis and a big reluctance in q-axis. Some of the following provisions will affect both reluctances, some have only an effect in one direction. All measures are applied in the rotor and will be shown at one magnetic pole in the following figures.

2.1 Air Gap Variation in PMSM

First method to affect the reluctances is a variation of the air gap length δ. $\delta(\alpha) = \delta_{min}$ at the d-axis, $\delta(\alpha) = \delta_{max}$ at he q-axis. This will affect L_d to a minor degree, but L_q to a great extent. As it will be shown later the function and amplitude of $\delta(\alpha)$ depends strongly on other measures to control the magnetic reluctance of the machine.

2.2 Placement of the Magnets

As, for the flux produced by the stator winding, the magnets behave in a magnetic way similar like air, it will be necessary to have magnets with a small height

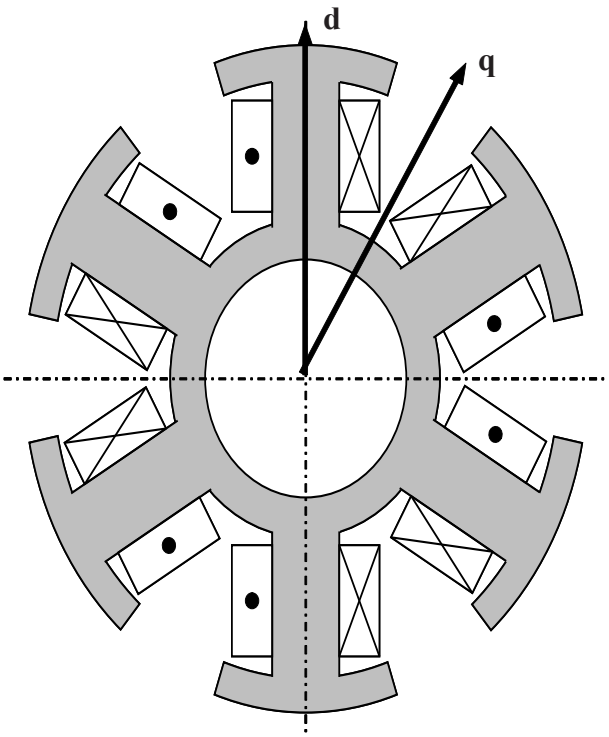

Figure 3: Salient poles in the rotor of a machine with a field excited by a field current

ISSN 2032-6653

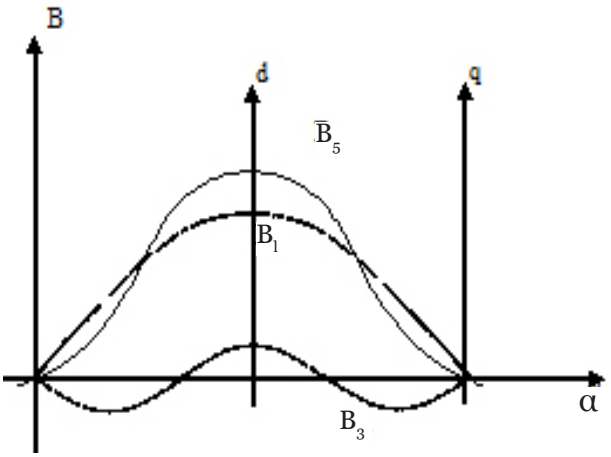

Figure 4: Flux-density distribution in the air gap of a machine with salient poles

h_M. To design a compact machine able to run at high speeds, it will be in need to bury the magnets in the rotor. As h_M should be as small as possible the magnets need to be arranged in a so called flux-concentration design. In Figure 6, two possible methods for a flux-concentration are shown. In both designs it has to be taken care that the magnetic shortcut at the ends of the magnets close to the center of the rotor are as small as possible.

In the design on the right of Figure 6 the magnets are split, so the q-axis lies in the gap of the two parts of the magnet. This can be utilized for a air gap variation like described in the paragraph above. For this purpose the magnet pole angle β_M is introduced as shown in Figure 7. The best angle β_M for this task can easily be calculated, for a machine with 3 phases.

$$\beta_M = \frac{2}{3} \cdot \frac{\pi}{p}$$, where p is the number pole pairs.

2.3 Conduction of the Magnetic Flux

In the rotor the magnetic flux can be guided by cut outs in the rotor iron which do not obstruct the magnetic flux due to the magnet and demagnetizing current, but will hinder the magnetic flux normal to that above mentioned flux as shown in Figure 8.

The cut outs at the end of the magnets have, beside their function to hinder the flux in the q-axis, to decrease the magnetic shortcut close to the air gap.

2.4 Combined Measures

To get the best result, we will have to combine all above

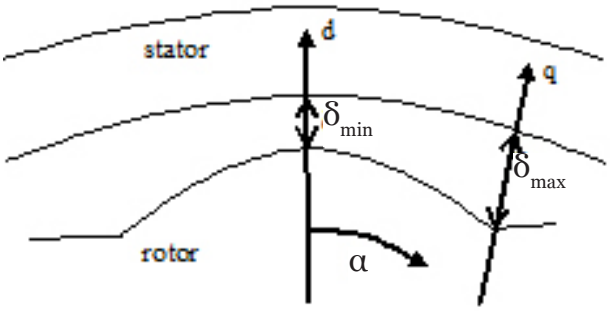

Figure 5: Air gap variation in a PMSM

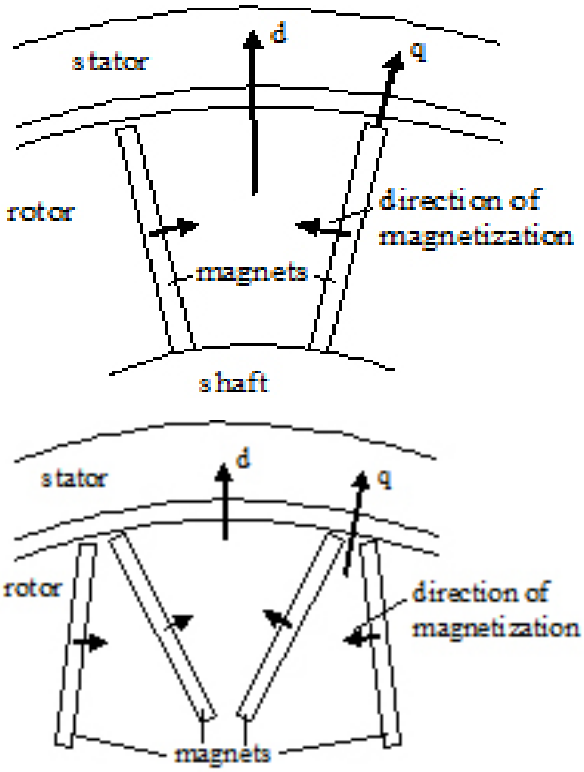

Figure 6: Flux-concentration

discussed arrangements. There are of course no known guidelines in which way those steps have to be taken, but some of the arrangements can be done by common sense. The maximum air gap length δ_{max} should be about two to three times δ_{min}. The width of the cut outs in the rotor iron should be about δ_{max}. The length of the cut outs depend more on mechanical premises.

ISSN 2032-6653

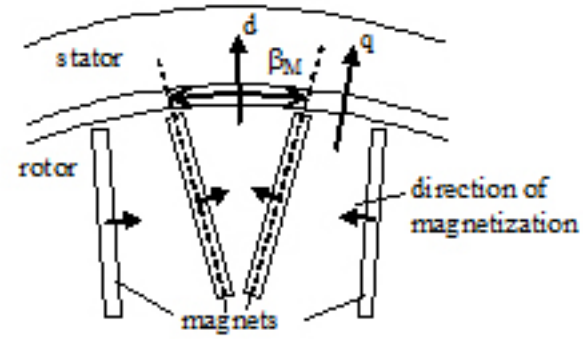

Figure 7: Variation of the magnet pole angle β_M

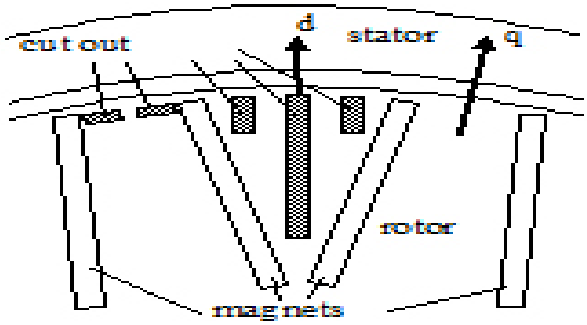

Figure 8: Cut outs in the rotor iron

3. MOTOR DESIGN AND RESULTS

3.1 Conditions for a Design

Further conditions for the machine design have been set to the following values:

Condition	Symbol	Value
Direct current link voltage	U_{ZK}	540 V
Rated power	P_N	50 kW
Rated torque	M_N	150 Nm
Spread		3200 – 6600 min^{-1}
Maximum speed	n_{max}	9900 min^{-1}
Stator diameter	d_S	250 mm
Stator length	l_S	250 mm

Table 2: Preconditions for a new PMSM for HEV

Another very important prerequisite for a PMSM is the behavior of the machine in case of errors. One of those errors is a short cut of all three phases of the machine. In this case the motor should stay in a thermal stable state at all times. This leads to the postulation, that the short cut current has not to exceed the rated current at any time under faulty conditions.

3.2 Machine Parameters

With those conditions a machine has been designed with the parameters laid out in Table 3.

3.3 Results

Some calculations will give an overview of the characteristics of this machine. First the magnetic behavior of the machine will be discussed on some FEM calculations, followed by analytical calculations of losses and efficiency at some operating points.

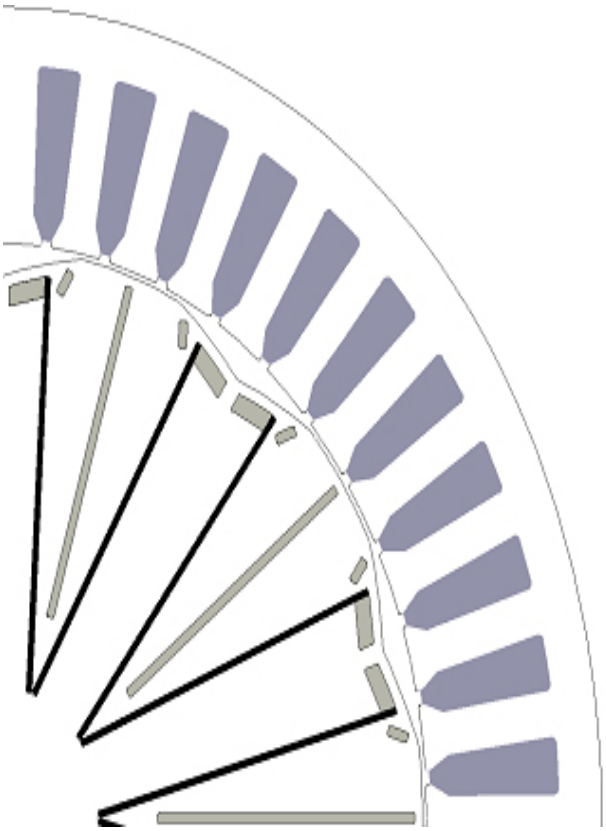

Figure 9: Cross section of a PMSM with $L_d > L_q$

3.3.1 FEM RESULTS

- Flux lines in the cross section
- Flux density distribution in the air gap

As predicted the 3rd harmonic of the flux density distribution has a negative sign in relation to the 1st harmonic. In the following spectral distribution it

ISSN 2032-6653

Parameter	Symbol	Value
Number of pole pairs	P	5
Rated power	P_N	60 kW
Rated torque	M_N	160 Nm
Rated current	I_{1N}	113 A
Utilization (Air gap sheer stress)	σ	18 kN/m²
Constant power range (electrically)		3200 – ∞ min^{-1}
Inductance in d-axis (no load)	L_d	1.030 mH
Inductance in q-axis (no load)	L_q	0.657 mH
Resistance of one phase	R_1	18.4 mΩ
Flux-linkage due to magnets	Ψ_M	0.144 Vs
Flux-density peak value (no load)	B_0	1.41 T
Mass of iron in the stator	m_S	22.52 kg

Table 3: Machine parameters of a PMSM for HEV

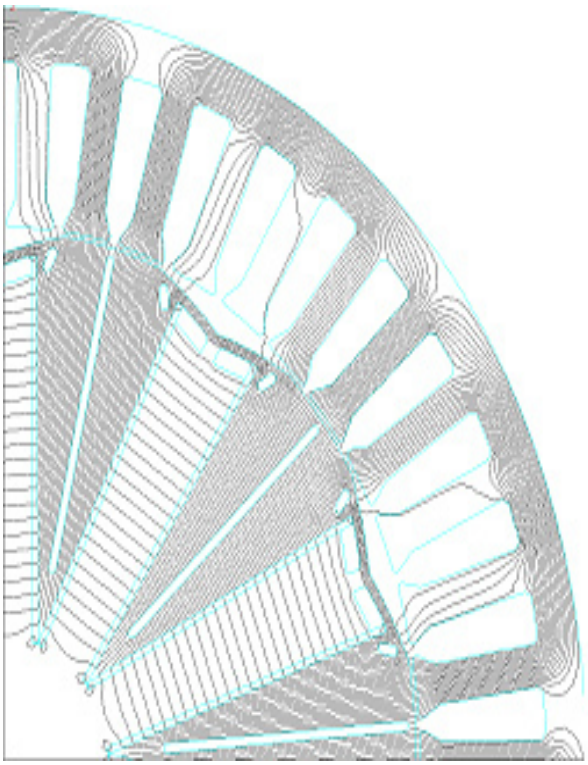

Figure 10: Flux lines at no load

shows up, that there are even harmonics existing, due to the special winding applied in the design.

3.3.2 ANALYTICAL RESULTS

The attention of the following examinations turns to losses and efficiency at several operating points.

The calculation includes iron losses and copper losses in the stator. For all operating points, different torque values at a given speeds, the best point, in a sense of minimum losses for those points, has been searched. All terms are supposed to be sinusoidal and all calculations are conducted for stationary conditions.

The copper losses satisfy the following equation:

$$P_{V,Cu} = 3 \cdot R_1 \cdot I_1^2 \text{ with } I_1 = \sqrt{I_d^2 + I_q^2}$$

I_d : RMS value of d-axis-current
I_q : RMS value of q-axis- current

For the iron losses the simplified "Steinmetz-equation" has been utilized:

$$P_{V,Fe} = m_S \cdot (c_h + c_e \cdot f) \cdot f \cdot B^2$$

c_h : specific hysteresis losses
c_e : specific eddy-current losses

ISSN 2032-6653

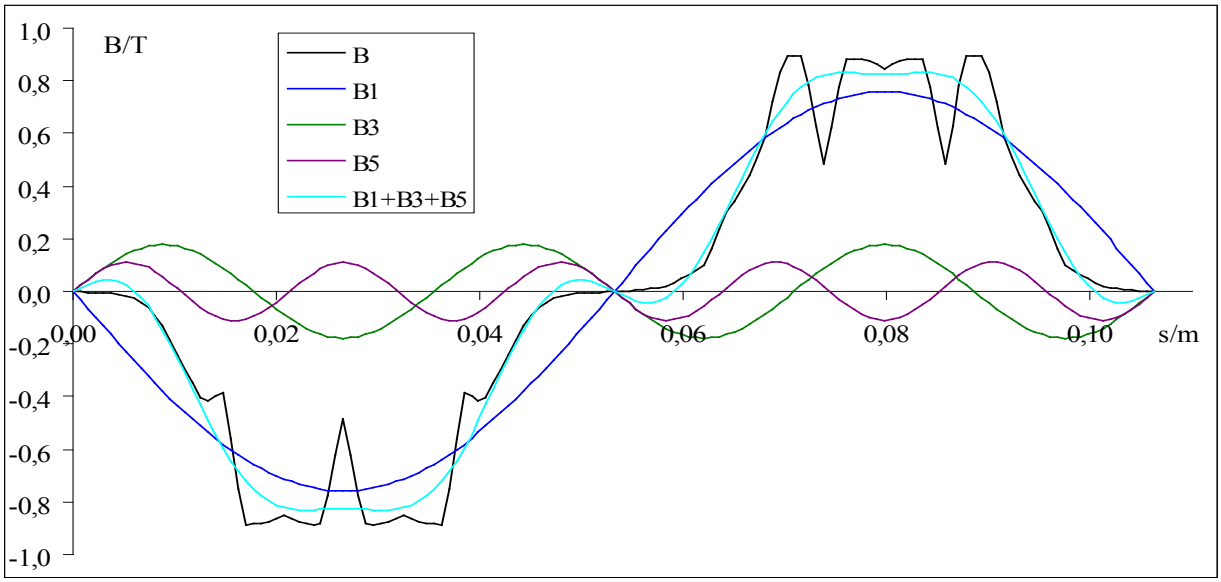

Figure 11: Flux density distribution at mid air gap, 1st 3rd 5th harmonic and sum of the harmonics

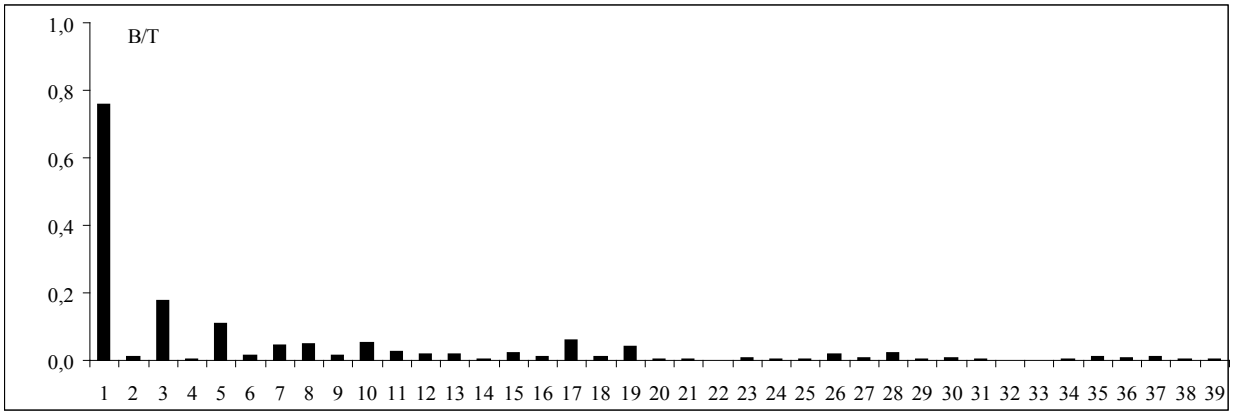

Figure 12: Harmonic distribution of the Flux density distribution at mid air gap

The calculation of specific losses is based on the method described in [2]. The material underlying this calculation is 3% Si Alloy of 0.35 mm thickness, which gives 2.33 W/kg specific iron loss at a electrical frequency of 50 Hz and a peak flux-density of 1,5 T.

To find the minimum of the sum of both losses at different operating points, the equation for torque has to be introduced:

$$M = 3 \cdot p \cdot \left(\Psi_M + \left(L_d - L_q\right) I_d\right) I_q$$

This equation can be solved for I_d:

$$I_d = \frac{M}{3 \cdot p \cdot \left(L_d - L_q\right) I_q} - \frac{\Psi_M}{\left(L_d - L_q\right)}$$

For B in the "Steinmetz-equation" the following projection, which has its fundament in measurement data on readings on the above mentioned material, has been performed:

$$B^2(I_d, I_q) = \left[\left(\Psi_M + L_d \cdot I_d\right)^2 + \left(L_q \cdot I_q\right)^2\right] \frac{B_0^2}{\Psi_M^2}$$

This gives for the sum of the losses:

$$P_V = 3 \cdot R_1 \cdot \left(I_d^2 + I_q^2\right) + m_S \cdot \left(c_h + c_e \cdot f\right) \cdot f \cdot \left[\left(\Psi_M + L_d \cdot I_d\right)^2 + \left(L_q \cdot I_q\right)^2\right] \frac{B_0^2}{\Psi_M^2}$$

Inserting I_d into this equation results:

ISSN 2032-6653

$$P_V = 3 \cdot R_1 \cdot \left(\left(\frac{M}{3 \cdot p \cdot \left(L_d - L_q\right) I_q} - \frac{\Psi_M}{\left(L_d - L_q\right)} \right)^2 + I_q^2 \right)$$

$$+ m_S \cdot \left(c_h + c_e \cdot f\right) \cdot f \cdot \frac{\left(\Psi_M + L_d \left(\frac{M}{3 \cdot p \cdot \left(L_d - L_q\right) I_q} - \frac{\Psi_M}{\left(L_d - L_q\right)} \right) \right)^2 + \left(L_q \cdot I_q\right)^2}{\Psi_M^2} B_0^2$$

Setting $\frac{dP_V}{dI_q} = 0$ and solving for I_q will give I_q and I_d for the minimum of losses at all operating points.

Applying the current values to the modified "Steinmetz-equation" finally provides the losses at any operating point.

These calculations have been carried out for torque increasing in steps of 20 Nm and speeds increasing in steps of 600 rpm. In Figure 13, lines of constant torque are plotted over speed.

For the above mentioned grid of operating points the efficiency of the motor has been determined and is shown in Figure 14 as a plot of equidistant lines over the grid of operating points.

The high values of the efficiency are due to the absence of additional rotor losses and friction in the calculation and for the calculation of copper losses in a presumed temperature of 20° C . Adding all those losses and calculating at realistic conditions, the efficiency will decrease about 3% to 5% at the best point. The motivation not to include those losses lies in the more exact to perform comparison of two machines of the same rated power with complete different designs, as it will be carried out in the next chapter.

4. ADVANTAGES OF THE NEW DESIGN

To see the gain of this design it will be useful to compare it with a motor which is typical for PMSM in HEV. In machines of that kind magnets are buried and usually $L_q > L_d$ is fulfilled. In order to achieve a fair comparison to known machine layouts, a design of a machine has been carried out with the same dimensions and materials, the same winding, the same rated power and the same rated torque.

The calculations mentioned above have been repeated for the conventional design. The differences in losses and efficiency are shown in Figures 15 and16. It is obvious, that the new design will be more efficient at higher speeds and low loads.

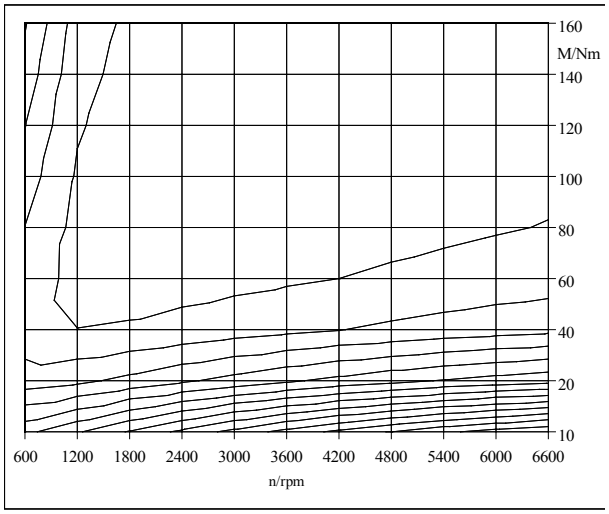

Figure 14: Efficiency at various operating points

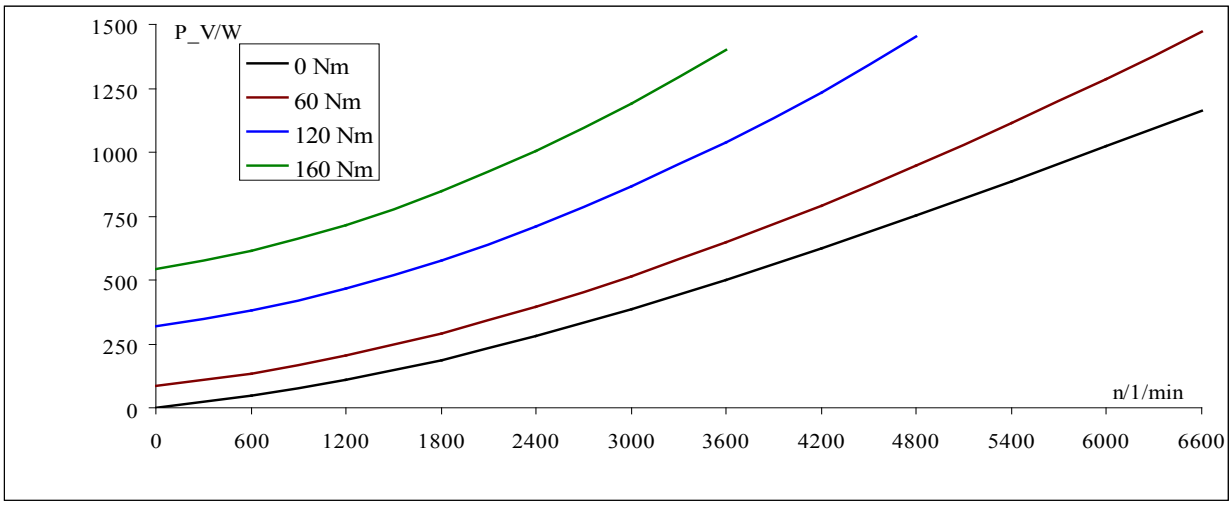

Figure 13: Sum of copper and iron losses in the stator at specific loads

ISSN 2032-6653

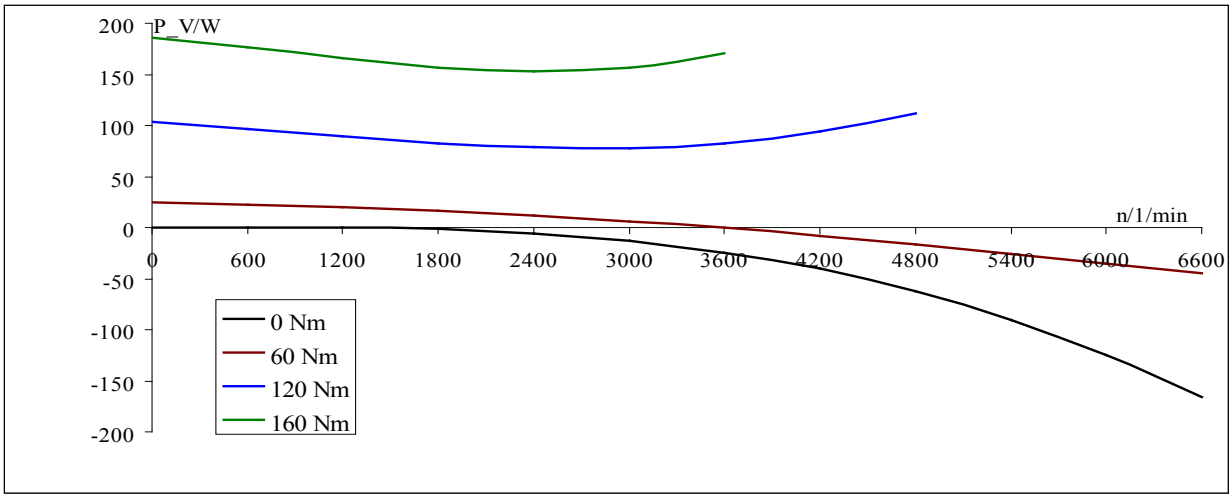

Figure 15: Differences in losses at various operating points ($P_{V,new}$ - $P_{V,conventional}$)

Parameter	Symbol	Value
Inductance in d-axis (no load)	L_d	0.790 mH
Inductance in q-axis (no load)	L_q	1.581 mH
Flux-linkage due to magnets	Ψ_M	0.168 Vs
Flux-density peak value (no load)	B_0	1.42 T
Mass of iron in the stator	m_S	21.92 kg

Table 4: Machine parameter of a conventional PMSM for HEV

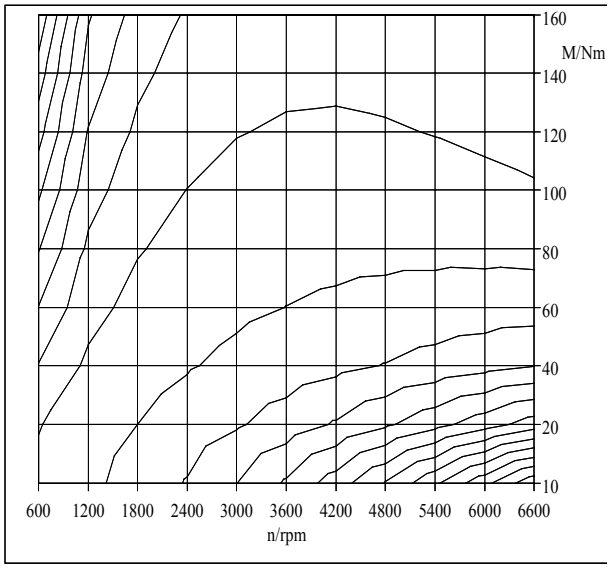

Figure 16: Differences in efficiency at various operating points ($\eta_{V,new}$ - $\eta_{V,conventional}$)

REFERENCES

[1] J. Ranneberg, Y. Tadros, U. Schäfer. Motor-inegrated circular converter for hybrid vehicles. EPE Journal Vol. 14 no. 2, March, April, May 2004.

[2] T.J.E. Miller. SPEED's Electric Motors. University of Glasgow, 2002.

[3] Y. Zhang, X. Wen, J. Chen. The Stator Current optimization of Interior Permanent Magnet Synchronous Motor for Electric Vehicle. EVS-18, Berlin 2001.

[4] Kogura, Kawabata, Yamada, Kanamori. Development of Motor Control Technology for Electric Vehicles. EVS-14, Orlando 1997.

AUTHORS

Dipl.-Ing. Uwe Vollmer has been employed at the TU Berlin, Department of Electrical Drive Technology, since 2006. From 2004 to 2006 he worked as Electrical Engineer at the University of Stuttgart, where he received a diploma in Electrical Engineering in 2002. From 2000 to 2004, he planned technical equipment of theaters. Phone: 49-30-31425506, uwe.vollmer@iee.tu-berlin.de.

U. Schäfer received his diploma and PhD in Electrical Engineering in 1985 and 1989, respectively, from RWTH Aachen, Germany. He then joined AEG from 1990 until 1994. From 1994 to 2003 he was with DaimlerChrysler AG as Research Manager for electrical drives. From 2004 to 2006, he was a professor of Electrical Energy Conversion at the University of Stuttgart. Since 2006, he has been head of the Department of Electrical Drive Technology, TU Berlin, Germany, and since 2007 Vice President of DGES. His main research interests include electrical propulsion for rail and road application, as well as energy efficient electric drives. Phone: 49-30-31423372.